Giant negative magnetoresistance in the layered semiconductor $CeTe_{2-x}Sb_x$ with variable magnetic polaron density

H. Murakawa,[1,*] Y. Nakaoka,[1] K. Iwase,[1] T. Kida,[2] M. Hagiwara,[2] H. Sakai,[1] and N. Hanasaki[1,3]

[1]*Department of Physics, Osaka University, Toyonaka, Osaka 560-0043, Japan*

[2]*Center for Advanced High Magnetic Field Science (AHMF), Graduate School of Science, Osaka University, Toyonaka, Osaka 560-0043, Japan*

[3]*Spintronics Research Network Division, Institute for Open and Transdisciplinary Research Initiatives, Osaka University, Suita, Osaka 565-0871, Japan*

(Received 7 February 2023; accepted 5 April 2023; published 24 April 2023)

We report that the layered semiconductors $CeTe_{2-x}Sb_x$ with low charge carrier density $\leqslant 2 \times 10^{18}$ cm^{-3} exhibit giant negative magnetoresistance exceeding two digits at 2 K. The drastic decrease in electrical resistivity is induced by the transition from the antiferromagnetic to the forced-ferromagnetic state with a wide range of electrical resistivities [approximately 20 to (3×10^7) Ω cm] in zero magnetic field. In contrast, the negative magnetoresistance almost disappears in the low-resistivity sample with much higher carrier density ($\sim 2.4 \times 10^{20}$ cm^{-3}). These results indicate that the observed giant magnetoresistance is driven by a substantial change in the mobility of the magnetic polarons. In $CeTe_{2-x}Sb_x$, the charge carrier density is variable by several digits by the substitution of Te with Sb. Consequently, the giant negative magnetoresistance is preserved within a wide range of electrical resistivity as long as the magnetic polaron density is low enough that the magnetic polarons rarely overlap each other. The magnetic polaron diameter is discussed using the samples' carrier density.

DOI: 10.1103/PhysRevB.107.165138

I. INTRODUCTION

A significant change in the electrical resistivity ρ of materials as a response to an external magnetic field H demonstrates advantages for the application to sensing and switching devices [1]. This phenomenon, i.e., giant magnetoresistance, is observed in various materials, and several mechanisms are involved with this phenomenon [2–5]. In a magnetic field, a compensated semimetal shows a dramatic increase in electrical resistivity, reaching several digits at low temperatures due to the cancellation of Hall voltage [6,7], while most of the magnetic conductors show a decrease in resistivity (negative magnetoresistance) through the interaction between local magnetic moments and itinerant electrons [8–18]. Although there are various types of giant magnetoresistance materials, it is difficult to widely tune the range of the electrical resistivity in the same series of compounds, since it is primarily determined by the total number of inside charge carriers. For instance, the electrical resistivity of metallic compounds with the large amount of charge carriers is insensitive to carrier doping. Furthermore, the electrical resistivity range for materials showing giant magnetoresistance is limited, although the electrical resistivity in Mott insulators is sensitive to finite carrier doping [8].

Contrary to these systems, magnetic semiconducting materials with low carrier density are promising. In materials with low-density electrical charge carriers, the formation of quasiparticles, i.e., polarons, tends to reduce the mobility of charge carriers, since polarons induce a local lattice deformation to gain an electrostatic energy by the electron-phonon coupling. Similarly, a quasiparticle generated by the magnetic interaction between surrounding magnetic moments is called a *magnetic polaron*, forming local ferromagnetic clusters to gain exchange energy [19]. In contrast to the lattice polaron, the mobility of magnetic polarons is controllable by the external magnetic field to align local magnetic moments. Therefore electrical resistivity decreases with increasing magnetization and saturates in the forced-ferromagnetic state. Moreover, the magnitude of magnetoresistance, originating from the mobility change in the magnetic polaron, should be preserved in a wide range of electrical resistivity as long as the magnetic polaron density is low enough that the magnetic polarons rarely overlap each other. Although several compounds have been reported to display huge magnetoresistance exceeding several digits using this mechanism [20,21], an examination of the effect of the carrier density on the magnitude of the magnetoresistance has been lacking, and the relationship between magnetization and electrical resistivity in the entire variation process of the magnetization up to the forced-ferromagnetic state has rarely been reported [22].

In this paper, we report that the layered semiconductors $CeTe_{2-x}Sb_x$ with low charge carrier density $\leqslant 2 \times 10^{18}$ cm^{-3} exhibit a significant decrease in the electrical resistivity exceeding two digits at 2 K over a wide range of zero-field electrical resistivities. In these samples, we observed a remarkable relationship between magnetization and electrical resistivity up to the forced-ferromagnetic state at various temperatures. In contrast, the negative magnetoresistance becomes significantly smaller (≈3% at 9 T at 2 K) in the sample

*Corresponding author: murakawa@phys.sci.osaka-u.ac.jp

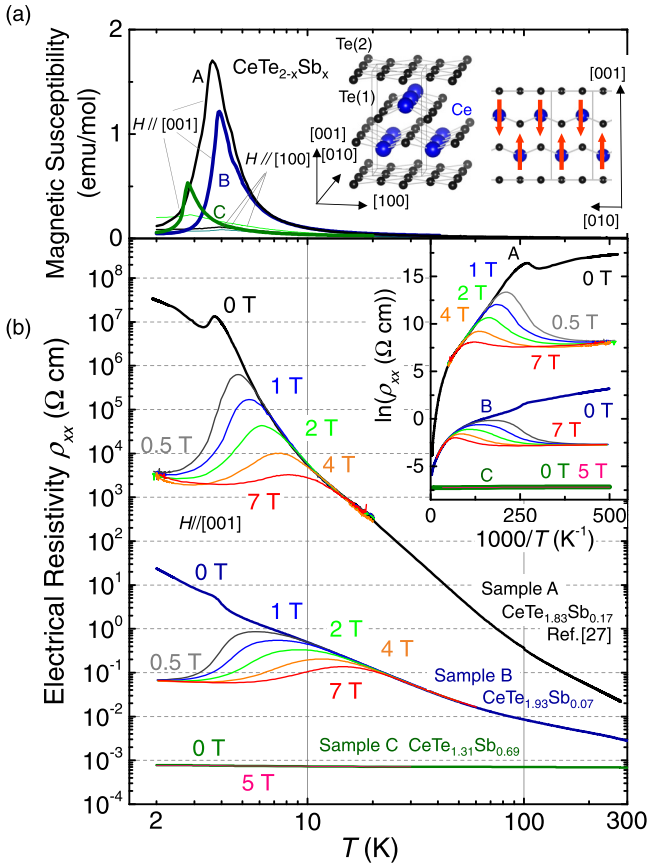

FIG. 1. Temperature dependence of (a) magnetic susceptibility at 0.1 T and (b) electrical resistivity ($I \parallel [100]$) of samples A ($CeTe_{1.83}Sb_{0.17}$), B ($CeTe_{1.93}Sb_{0.07}$), and C ($CeTe_{1.31}Sb_{0.69}$) down to 2 K in various magnetic fields along [001]. For the electrical resistivity of sample A, the data in Ref. [27] are employed. The inset in (a) shows the crystal structure and the magnetically ordered state at the lowest temperature at 0 T. The inset in (b) shows the Arrhenius plots of the electrical resistivities of the three samples.

with much higher carrier density ($\approx 2.4 \times 10^{20}$ cm^{-3}). These results offer strong evidence that the magnetic polaron mechanism is responsible for the giant negative magnetoresistance in this system.

II. EXPERIMENT

Single crystals of $CeTe_{2-x}Sb_x$ ($x = 0.07$, 0.17, and 0.69) were obtained by the chemical vapor transport technique with iodine as a transport agency. Single-crystal x-ray diffraction was employed to analyze the layered structure consisting of the magnetic insulating [CeTe(1)] layer and the semiconducting Te(2) layers [inset in Fig. 1(a)]. The inductively coupled plasma method accurately determined the composition ratio of each element. The electrical resistivity was measured using the four-probe method. The gold paste was used for putting the gold wire to the sample. We labeled the samples as samples A, B, and C in the order of magnitude of the electrical resistivity at 0 T (from high to low).

III. RESULTS AND DISCUSSION

Figure 1(a) shows the magnetic susceptibility of the three samples, samples A ($x = 0.17$), B ($x = 0.07$), and C ($x = 0.69$), in $H \parallel [001]$ and $H \parallel [100]$. The steep increase in the susceptibility in $H \parallel [001]$ below 10 K indicates the development of the ferromagnetic correlation between intraplane Ce ions with a magnetic easy axis along [001]. In addition, the sharp decrease below ~2.8–4.0 K reflects the interplane antiferromagnetic order as discussed in previous reports [23–27]. Figure 1(b) shows the temperature dependence of the electrical resistivities of the three samples in various magnetic fields along the [001] direction. At 0 T, two samples, samples A and B, demonstrate the semiconducting behavior in the entire temperature range below 300 K, but their electrical resistivity values differ significantly. The resistivities of sample B are one digit lower at 300 K and six digits lower at 2 K than those of sample A. In contrast, the electrical resistivity in the most conducting sample, sample C, is nearly temperature independent. From the Hall resistivity measurements, carrier density in samples B and C was calculated to be $\sim 2 \times 10^{18}$ cm^{-3} (electrons) and $\sim 2.4 \times 10^{20}$ cm^{-3} (holes), respectively, at 2 K [28], but it could not be determined in sample A because of the significantly higher longitudinal resistivity. Therefore the carrier density of sample A is considered to be much lower than the other two samples and in the vicinity of the dilute limit [29]. Note that only a small number of the doped carriers contribute to the electrical conduction due to the energy gap of the charge-density-wave state [25–27,30–33]. Below 10 K, the electrical resistivity in samples A and B exhibits significant magnetic field dependence, but not in sample C.

Figures 2(a) and 2(b) show the magnetization and electrical resistivity, respectively, of the three samples in $H \parallel [001]$ up to 2 T at 2 K. The semiconducting samples A and B show a significant decrease in the electrical resistivity in $H \parallel [001]$ above the ferromagnetic transitions. Notably, these two samples show similar temperature and magnetic field dependences except for their zero-field resistivity value, as if these were shifted vertically in the logarithmic display. In contrast, the negative magnetoresistance is negligibly small in the most conducting sample C with much higher carrier density. This result is consistent with the magnetic polaron mechanism; the magnitude of the magnetoresistance is determined by the mobility change in the polaron, and the electrical resistivity value depends on the charge carrier density [34]. Assuming that the magnetic polaron density n of sample A is inversely proportional to the magnitude of the electrical resistivity in the forced-ferromagnetic state at 0.4 T and the average distance between magnetic polarons is $n^{-\frac{1}{3}}$, we plot $\rho(0\ \mathrm{T})/\rho(0.4\ \mathrm{T})$ as a function of $n^{-\frac{1}{3}}$ in the inset in Fig. 2(b). Here, $n^{-\frac{1}{3}}$ is 3300, 80, and 17 Å for samples A, B, and C, respectively. Therefore the magnetic polaron diameter ξ is estimated to be $17 < \xi < 80$ Å in the isotropic three-dimensional model.

Next, we discuss the strong relationship between magnetization and electrical resistivity in the low-temperature range, which captures the crucial characteristic of the magnetic polaron mechanism. As a prototypical example, we show the magnetization and electrical resistivity of sample B ($CeTe_{1.93}Sb_{0.07}$) at 2 K in the low-magnetic-field range in Figs. 3(a) and 3(b), respectively. Those of samples

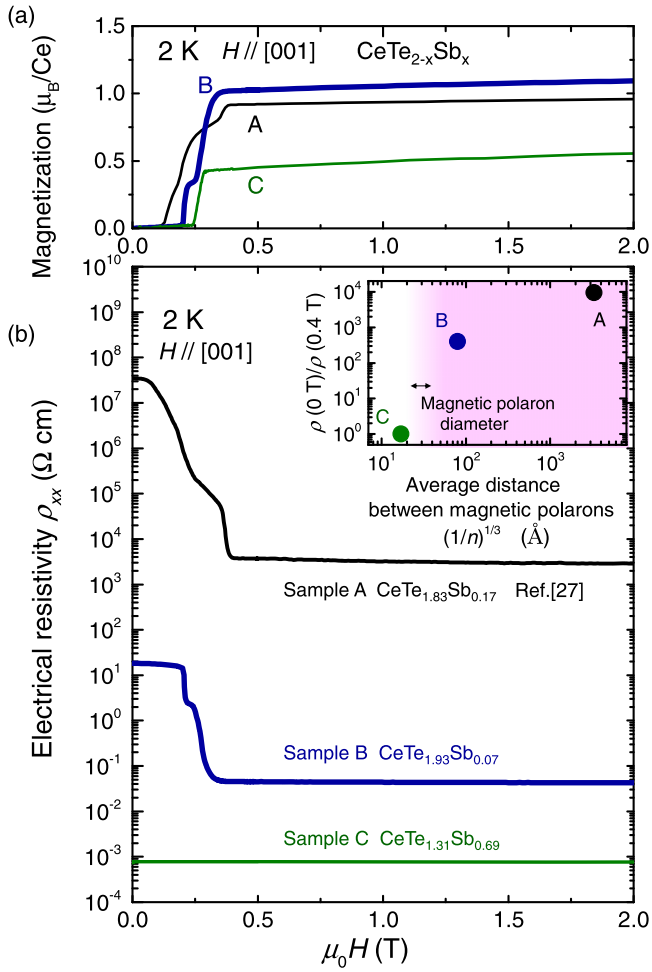

FIG. 2. Magnetic field dependence of (a) magnetization and (b) electrical resistivity ($I \parallel [100]$) of samples A ($CeTe_{1.83}Sb_{0.17}$), B ($CeTe_{1.93}Sb_{0.07}$), and C ($CeTe_{1.31}Sb_{0.69}$) at 2 K in a magnetic field along [001]. The inset shows the magnetoresistance $[\rho(0\ \mathrm{T})/\rho(0.4\ \mathrm{T})]$ as a function of the average distance between the charge carriers estimated as $n^{-\frac{1}{3}}$.

A and C are discussed in Ref. [27] and the Supplemental Material, respectively. In $CeTe_{1.93}Sb_{0.07}$, the interplane antiferromagnetic order occurs below 4.0 K, and thus the magnetization approaches nearly zero after cooling at zero fields. In the magnetic-field-increasing process, the magnetization suddenly jumps at 0.2 T and reaches around 1/3 of its saturation value M_{sat}, and it steeply increases again from 0.25 T up to 0.35 T. After that, the magnetization almost saturates in the forced-ferromagnetic state. The observed step structure in the magnetization suggests the collective reorientation of the in-plane ferromagnetic moments, and the $\sim 1/3 M_{\mathrm{sat}}$ at the first jump might be induced by the flip of magnetic moments per three layers, such as up-up-down magnetic stacking along the c axis at 0.2 T [35]. Corresponding to the variation in the magnetization, the electrical resistivity of sample B ($CeTe_{1.93}Sb_{0.07}$) drastically changes during the first jump at 0.2 T $[\rho(0.2\ \mathrm{T})/\rho(0\ \mathrm{T}) = 1/7.5]$ and then further decreases at the second jump $[\rho(0.35\ \mathrm{T})/\rho(0.2\ \mathrm{T}) = 1/54]$. In the forced-ferromagnetic state above 0.35 T, the electrical resistivity is essentially constant up to 7 T. Therefore the

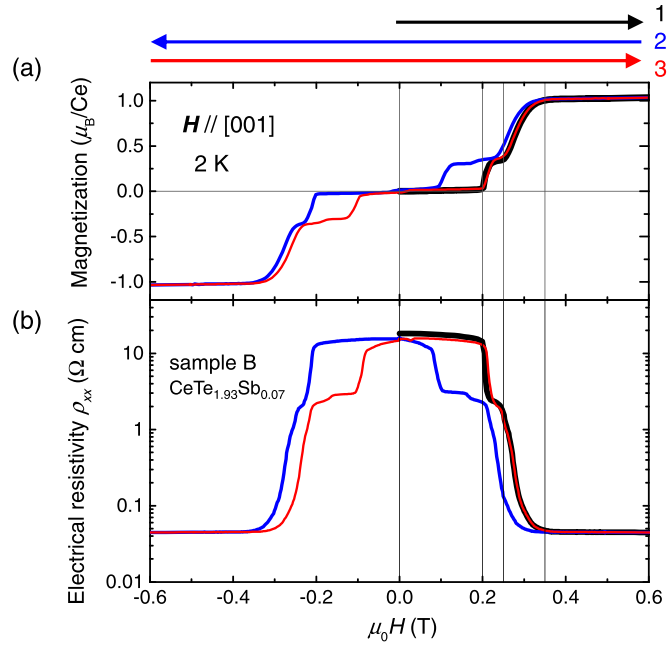

FIG. 3. (a) Magnetization and (b) electrical resistivity of sample B ($CeTe_{1.93}Sb_{0.07}$) at 2 K in the low-magnetic-field range along [001]. The color (black, blue, and red) indicates the procedure of applying the magnetic field.

negative magnetoresistance $\rho(0.35\ \mathrm{T})/\rho(0\ \mathrm{T})$ reaches 1/405 in sample B through the transition from the antiferromagnetic state to the forced-ferromagnetic state. Interestingly, the mobility of charge carriers in the quasi-two-dimensional system is significantly dependent on the long-range interlayer antiferromagnetic order.

A strong relationship between the magnetization and electrical resistivity of sample B ($CeTe_{1.93}Sb_{0.07}$) is seen even above the antiferromagnetic transition temperature ($T_{\mathrm{N}} = 4.0$ K). Figures 4(a) and 4(b) show the magnetization and the electrical resistivity measured at various temperatures in $H \parallel [001]$, respectively. Below 10 K, the electrical resistivity substantially decreases with increasing magnetization. Figure 4(c) shows the electrical resistivity as a function of the magnetization in $H \parallel [001]$, obtained by the data in Figs. 4(a) and 4(b). The electrical resistivities at various temperatures nicely approach a constant value when the magnetization gets close to saturation. This is clear evidence of the existence of magnetic polarons in this compound.

Figures 5(a) and 5(b) show the magnetization and the electrical resistivity in $H \parallel [100]$ along the magnetic hard direction. In contrast to the case in $H \parallel [001]$, the magnetization gradually increases and does not reach the saturation value even at 7 T at 2 K. Correspondingly, the decrease in the electrical resistivity is moderate, and the value at 7 T at 2 K is ≈ 10 times higher than that in $H \parallel [001]$. The large anisotropy in the magnetization has been discussed on the basis of the anisotropic interlayer p-f mixing model [34]. Here the ground state of the Ce $4f$ orbit in the magnetic layers is determined by the symmetry of the unoccupied Te $5p$ orbits ($j_z = \pm\frac{3}{2}$) in the conduction layers. Figure 5(c) shows the electrical resistivity as a function of magnetization in

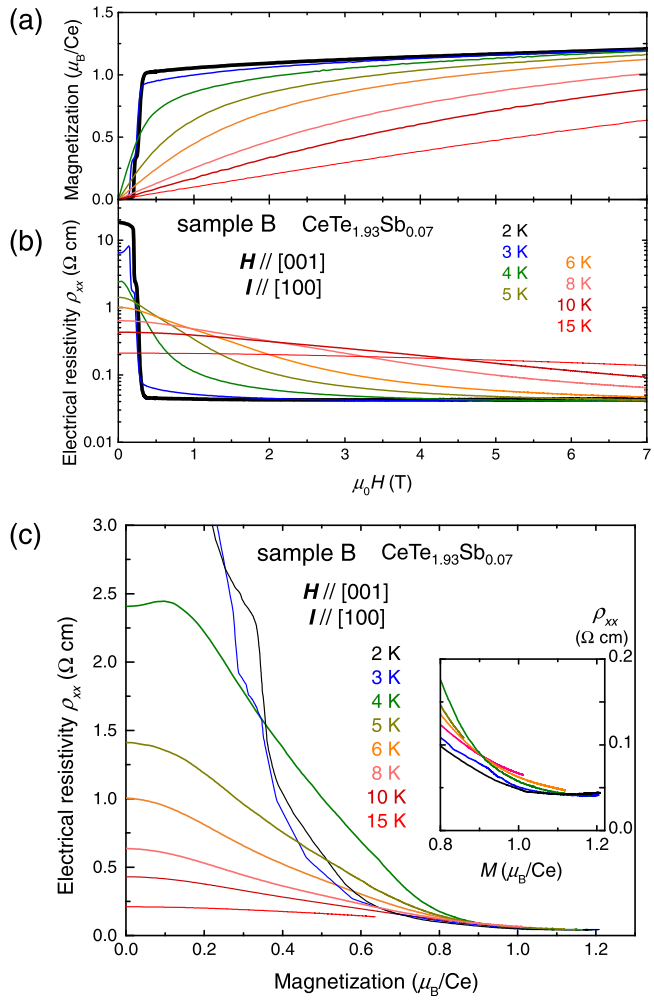

FIG. 4. (a) Magnetization and (b) electrical resistivity of sample B ($CeTe_{1.93}Sb_{0.07}$) at various temperatures in $H \parallel [001]$. (c) Electrical resistivity as a function of the magnetization, in which the data in (a) and (b) are used. The inset shows the magnified view to clarify the saturation in the forced-ferromagnetic state.

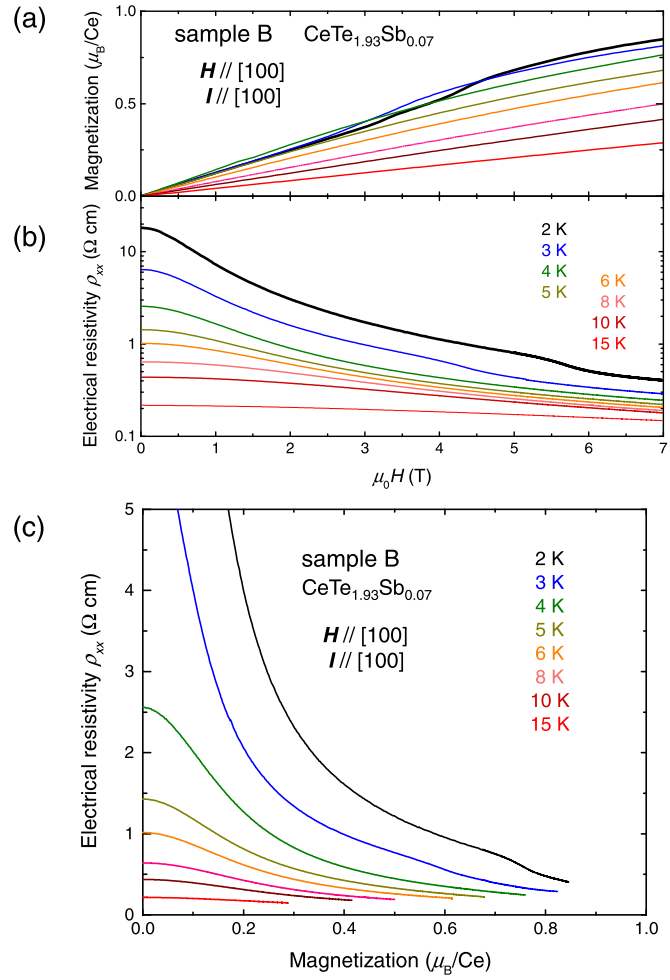

FIG. 5. (a) Magnetization and (b) electrical resistivity of sample B ($CeTe_{1.93}Sb_{0.07}$) at various temperatures in $H \parallel [100]$. (c) Electrical resistivity as a function of the magnetization, in which the data in (a) and (b) are used.

$H \parallel [100]$. Although the approach of the electrical resistivity is rather insufficient due to the unsaturated magnetization, the relationship is essentially the same as the case of $H \parallel [001]$. These results demonstrate that the doped charge carrier by chemical substitution, at least up to 2×10^{18} cm^{-3}, strongly interacts with the local magnetic moment and produces a magnetic polaron in $CeTe_{2-x}Sb_x$. The layered structure with large hybridization between the Ce $4f$ orbit in the magnetic layer and the Te $5p$ orbit in the conduction layer is considered the key for the tunable magnetic polaron density and resultant giant negative magnetoresistance.

IV. CONCLUSIONS

In conclusion, we have observed a strong relationship between magnetization and electrical resistivity in the layered semiconductors $CeTe_{2-x}Sb_x$ with a low carrier density $\leqslant 2 \times 10^{18}$ cm^{-3} and discovered that the electrical resistivities at various temperatures approach asymptotically to a constant value in the forced-ferromagnetic state. Furthermore, we demonstrated that the charge carrier density is controllable by chemical substitution in $CeTe_{2-x}Sb_x$. As a consequence, a significant decrease in the electrical resistivity exceeding two digits was observed over a wide range of electrical resistivities of around six digits in the sample with the lower carrier density, while the negative magnetoresistance almost disappears in the sample with higher carrier density of 2.4×10^{20} cm^{-3}. These results indicate that the magnetoresistance in $CeTe_{2-x}Sb_x$ is caused by the mobility change of a magnetic polaron and the huge amplitude of magnetoresistance is preserved as long as the magnetic polaron density is low enough that the magnetic polarons rarely overlap each other.

ACKNOWLEDGMENTS

This work was in part supported by JSPS KAKENHI Grants No. JP21K03445, No. JP21H00147, No. JP22H00109, and No. JP22K18689, the Murata Science Foundation, and the Asahi Glass Foundation. This work was carried out at the Center for Advanced High Magnetic Field Science at Osaka University under the Visiting Researcher's Program of the Institute for Solid State Physics, The University of Tokyo.

[1] M. N. Baibich, J. M. Broto, A. Fert, F. Nguyen Van Dau, F. Petroff, P. Etienne, G. Creuzet, A. Friederich, and J. Chazelas, Phys. Rev. Lett. **61**, 2472 (1988).

[2] A. B. Pippard, *Magnetoresistance in Metals* (Cambridge University Press, Cambridge, 1989).

[3] A. P. Ramirez, J. Phys.: Condens. Matter **9**, 8171 (1997).

[4] E. Dagotto, T. Hotta, and A. Moreo, Phys. Rep. **344**, 1 (2001).

[5] Y. Tokura, Rep. Prog. Phys. **69**, 797 (2006).

[6] P. B. Alers and R. T. Webber, Phys. Rev. **91**, 1060 (1953).

[7] K. Yokoi, H. Murakawa, M. Komada, T. Kida, M. Hagiwara, H. Sakai, and N. Hanasaki, Phys. Rev. Mater. **2**, 024203 (2018).

[8] A. Urushibara, Y. Moritomo, T. Arima, A. Asamitsu, G. Kido, and Y. Tokura, Phys. Rev. B **51**, 14103 (1995).

[9] H. Kuwahara, Y. Tomioka, A. Asamitsu Y. Moritomo, and Y. Tokura, Science **270**, 961 (1995).

[10] N. Hanasaki, H. Tajima, M. Matsuda, T. Naito, and T. Inabe, Phys. Rev. B **62**, 5839 (2000).

[11] A. K. M. Akther Hossain, M. Seki, T. Kawai, and H. Tabata, J. Appl. Phys. **96**, 1273 (2004).

[12] K. Ueda, J. Fujioka, B.-J. Yang, J. Shiogai, A. Tsukazaki, S. Nakamura, S. Awaji, N. Nagaosa, and Y. Tokura, Phys. Rev. Lett. **115**, 056402 (2015).

[13] Z. Tian, Y. Kohama, T. Tomita, H. Ishizuka, H. T. Hsieh, J. J. Ishikawa, K. Kindo, L. Balents, and S. Nakatsuji, Nat. Phys. **12**, 134 (2016).

[14] J. Yin, C. Wu, L. Li, J. Yu, H. Sun, B. Shen, B. A. Frandsen, D.-X. Yao, and M. Wang, Phys. Rev. Mater. **4**, 013405 (2020).

[15] Y. Ni, H. Zhao, Y. Zhang, B. Hu, I. Kimchi, and G. Cao, Phys. Rev. B **103**, L161105 (2021).

[16] J. Seo, C. De, H. Ha, J. E. Lee, S. Park, J. Park, Y. Skourski, E. Sang, C. B. Kim, G. Y. Cho, H. W. Yeom, S. W. Cheong, J. H. Kim, B. J. Yang, K. Kim, and J. S. Kim, Nature (London) **599**, 576 (2021).

[17] Z. L. Sun, A. F. Wang, H. M. Mu, H. H. Wang, Z. F. Wang, T. Wu, Z. Y. Wang, X. Y. Zhou, and X. H. Chen, npj Quantum Mater. **6**, 94 (2021).

[18] H. Yang, Q. Liu, Z. Liao, L. Si, P. Jiang, X. Liu, Y. Guo, J. Yin, M. Wang, Z. Sheng, Y. Zhao, Z. Wang, Z. Zhong, and R. W. Li, Phys. Rev. B **104**, 214419 (2021).

[19] A. Mauger, Phys. Rev. B **27**, 2308 (1983).

[20] M. R. Oliver, J. O. Dimmock, and T. B. Reed, IBM J. Res. Dev. **14**, 276 (1970).

[21] P. Rosa, Y. Xu, M. Rahn, J. Souza, S. Kushwaha, L. Veiga, A. Bombardi, S. Thomas, M. Janoschek, E. Bauer, M. Chan, Z. Wang, J. Thompson, N. Harrison, P. Pagliuso, A. Bernevig, and F. Ronning, npj Quantum Mater. **5**, 52 (2020).

[22] K. Sugiyama, Y. Hirose, K. Enoki, S. Ikeda, E. Yamamoto, N. Tateiwa, Y. Haga, T. Kida, M. Hagiwara, K. Kindo, F. Honda, R. Settai, and Y. Onuki, J. Phys. Soc. Jpn. **80**, SA104 (2011).

[23] J. G. Park, I. P. Swainson, W. J. L. Buyers, M. H. Jung, and Y. S. Kwon, Physica B (Amsterdam) **241-243**, 684 (1998).

[24] J. G. Park, Y. S. Kwon, W. Kockelmann, M. J. Bull, I. P. Swainson, K. A. McEwen, and W. J. L. Buyers, Physica B (Amsterdam) **281-282**, 451 (2000).

[25] M. H. Jung, B. H. Min, Y. S. Kwon, I. Oguro, F. Iga, T. Fujita, T. Ekino, T. Kasuya, and T. Takabatake, J. Phys. Soc. Jpn. **69**, 937 (2000).

[26] M. H. Jung, K. Umeo, T. Fujita, and T. Takabatake, Phys. Rev. B **62**, 11609 (2000).

[27] H. Murakawa, Y. Nakaoka, T. Kida, M. Hagiwara, H. Sakai, and N. Hanasaki, Phys. Rev. Mater. **6**, 054604 (2022).

[28] See Supplemental Material at http://link.aps.org/supplemental/10.1103/PhysRevB.107.165138 for the Hall resistivity data in samples B and C.

[29] K. E. Lee, B. H. Min, J. S. Rhyee, J. N. Kim, J. H. Shim, and Y. S. Kwon, Appl. Phys. Lett. **101**, 143901 (2012).

[30] B. H. Min, E. D. Moon, H. J. Im, S. O. Hong, Y. S. Kwon, D. L. Kim, and H. C. Ri, Physica B (Amsterdam) **312-313**, 205 (2002).

[31] K. Y. Shin, V. Brouet, N. Ru, Z. X. Shen, and I. R. Fisher, Phys. Rev. B **72**, 085132 (2005).

[32] J. S. Kang, D. H. Kim, H. J. Lee, J. Hwang, H. K. Lee, H. D. Kim, B. H. Min, K. E. Lee, Y. S. Kwon, J. W. Kim, K. Kim, B. H. Kim, and B. I. Min, Phys. Rev. B **85**, 085104 (2012).

[33] E. Lee, D. H. Kim, J. D. Denlinger, J. Kim, K. Kim, B. I. Min, B. H. Min, Y. S. Kwon, and J. S. Kang, Phys. Rev. B **91**, 125137 (2015).

[34] T. Kasuya, M. H. Jung, and T. Takabatake, J. Magn. Magn. Mater. **220**, 235 (2000).

[35] R. Singha, T. H. Salters, S. M. L. Teicher, S. M. Lei, J. F. Khoury, N. P. Ong, and L. M. Schoop, Adv. Mater. **33**, 2103476 (2021).